Journal of the European Ceramic Society 20 (2000) 1739–1748

Adjustable biodegradation for ceramic fibres derived from silica sols

Mika Jokinen [a,*], Timo Peltola [b], Sinikka Veittola [c,1], Hanna Rahiala [a], Jarl B. Rosenholm [a]

[a] *Department of Physical Chemistry, Åbo Akademi University, Porthaninkatu 3-5, FIN-20500 Turku, Finland*
[b] *Institute of Dentistry, University of Turku, Lemminkäisenkatu 2, FIN-20520 Turku, Finland*
[c] *Fibre, Textile and Clothing Science, Tampere University of Technology, PO Box 589, FIN-33101 Tampere, Finland*

Received 15 February 1999; received in revised form 28 December 1999; accepted 30 January 2000

Abstract

Biodegradable silica fibres were prepared from TEOS-derived silica sols by dry spinning. The spinnability of the sols and its influence on the green state fibre structure were investigated. The same sols can be used to prepare different fibre structures depending on the process stage, temperature and viscosity. The spinning moment was found to be important in order to control the biodegradation. Influence of catalysts (HNO_3 and/or NH_3) as well as evaporation of the liquid on the process were investigated. They did not have an influence on the spinnability, but they reduced the overall reaction time. The prepared green state fibres were aged for 1 and 3 months indicating stable structure as a function of ageing time according to the biodegradation experiments, except in the case of high catalyst concentration. A porous structure was revealed using transmission electron microscopy. Heat-treatment of the fibres induced remarkable differences in the fibre bulk structure according to FT–IR measurements.

Keywords: Biodegradation; Fibres; SiO_2 fibres; Sol–gel methods; Spinning

1. Introduction

Sol–gel derived ceramic materials have many applications; bioceramics[1,2] is one of the most promising and interesting of these, although it still needs much development to optimise the materials properties in a biological environment. The sol–gel process, starting from the liquid phase, enables easy control of the pore structure and permits the introduction of other components to form different kinds of composites, especially in the case of silica-based materials. The processing of sol–gel derived silica fibres[3–17] is well known; the main parameter controlling the process is the functionality of the silica precursors, or the degree of branching of the silica clusters. The latter critically affects the spinnability and has commonly been characterised by rheological measurements. Various materials (also including other materials than silica) have been prepared and practical problems solved to develop the process; the most common applications are for optical and electronic purposes.[18–33]

Biomedical fibres of silica are novel materials and the flexibility of the sol–gel process creates possibilities to prepare various functional materials. The easy introduction of drugs and other related substances into the porous structure provides one example. Biodegradable and non-toxic biomedical materials that are able to work directly and locally in the human body would often be beneficial, for example as implants used as drug delivery devices or temporary implants in bone repairs. The sol–gel derived silica fibres can be prepared to fulfil these requirements.

The fibres have traditionally been used to improve the mechanical properties of materials. In the case of the sol–gel derived silica fibres, there are two main parameters determining the fibre bulk structure. By controlling the degree of branching of silica clusters, more or less condensed green fibre structures are achieved. The heat treatment of the fibres is another and more efficient way to condense the bulk structure. Depending on the application of the sol–gel derived biodegradable silica fibres, the optimum balance between mechanical properties and biodegradation may vary. If the fibres are used for drug delivery in soft tissue, the mechanical properties are of minor importance. However, the mechanical properties must allow processing of the obtained fibres to a desired form after spinning. If better mechanical properties are needed, it has to be

* Corresponding author at permanent address: University of Turku, Institute of Dentistry/Biomaterials Project, Lemminkaisenkatu 2, FIN-20520 Turku, Finland Tel.: +358-2-333-8325; fax: +358-2-333-8356.
E-mail address: mika.jokinen@utu.fi (M. Jokinen).
[1] Permanent address: The Patent Agency, Tampereen Patentitoimisto Oy, Hermiankatu 6, FIN-33720 Tampere, Finland

0955-2219/00/$ - see front matter
PII: S0955-2219(00)00036-4

remembered that biodegradation ceases after heat-treatment at high temperatures. The identification of the optimal mixture of mechanical properties and biodegradation is the main challenge for research.

The aim of this study was to prepare different alkoxy-derived biodegradable silica fibres using the sol–gel method by controlling the functionality of the silica precursor (tetraethyl orthosilicate, TEOS) and the structure of the polymeric silica clusters. Both the sols and the green state fibres were characterised to determine factors in the fibre bulk structure that define the fibre solubility (biodegradation) in a simulated body fluid. The silica cluster structure, depending both on the precursor concentrations and the sol–gel process stage, was chosen as the most important factor in the control of the properties of different fibres. Fine adjustment of recipes, including variations in TEOS/water ratios and usage of catalysts (acid or acid/base), is performed to control the cluster structure. The linear cluster structures and spinnability of the sol are sensitive to minor changes in pH and alkoxy/water ratio. Another factor utilised in this work, is the time-dependent behaviour of clusters in the sol–gel process. In acidic sols the polymerisation of the silica clusters proceeds spontaneously without interruption. The sol is spinnable over a certain time period rather than at a single point, which provides possibilities to prepare fibres having different properties but using the same recipe. The sols are characterised by rheological measurements; the green state fibres are studied with thermogravimetric analysis and with solubility tests in a simulated body fluid. FT–IR measurements are made on the fibres heat-treated in the thermogravimetric analysis. Transmission electron microscopy (TEM) is used to illustrate the inner bulk structure of the green body of the fibre.

2. Materials and methods

2.1. Sols for spinnability tests and rheological measurements

The silica sols were prepared from TEOS (tetraethyl orthosilicate 98%, ALDRICH, 13-190-3), deionised water (conductivity ~0.05 μS) and ethanol (Aa, 99.5%, Primalco Ltd, Finland); HNO_3 (65%, Merck, 456) or NH_3 (28%, Fluka, 09858) were used as catalysts in the sol–gel method. The molar ratios used are shown in Table 1 together with sample codes. The sols were stirred for 2 min and poured into test tubes (LP-111010 and LP116134, Prolab Oriola Ltd, Finland) which were closed tightly. The test tubes were placed into a water bath and the temperature was kept constant at 40°C. The preparation of FIB3 had an additional step. NH_3 was added into the sol after 24 h of aging at 40°C. The sol was vigorously stirred for 2 min. After stirring, the sol was immediately put back into the water bath.

Table 1
Sol compositions in molar ratios

Name	$r = H_2O$/TEOS	EtOH/TEOS	HNO_3/TEOS	NH_3/TEOS
FIB1 (A and B)	2	1	0.037	0
FIB2 (A and B)	2	1	0.1	0
FIB3	2	1	0.1	0.01

The spinnability of the three prepared samples (FIB1, FIB2 and FIB3) was first characterised visually (in situ at 40°C until the sols were spinnable and after that at room temperature) using a thin glass rod for drawing the sols. The rod was put into the sol and quickly drawn upwards. If the sol followed the rod forming a continuous fibre-like structure, the sol was considered to be spinnable.

Rheological characterisation of sols was carried out with a BOHLIN VOR Rheometer (C25) with concentric, coaxial cylinders and with a capillary viscometer of Ubbelohde -type (gravity force viscometer). A concept of relative gel time (t/t_{gel}) is used to describe process stages before the gel point. At the gel point, $t/t_{gel} = 1$. The aim was to measure the reduced viscosity in order to find out the viscosity dependence on the silica concentration. It is typical that linear polymeric cluster structures (suitable for spinning) are dependent on the polymer concentration. Samples were taken from the sols at different relative gelation times and diluted to four different concentrations with ethanol. Ethanol was considered to be a suitable solvent since it is one of the reaction products and it inhibits, or in greater amounts, practically prevents further reactions in the sol. The viscosity was measured immediately after dilution starting from the solution having the highest concentration of silica. The viscosity of ethanol (which is known) was measured after the sample measurements in order to check that the rheometers worked properly. Using the results obtained, the reduced viscosity (η_{sp}/C) was determined. The relative viscosity (η_{rel},) was taken as the ratio between the viscosity of the sample sol (η) and viscosity of ethanol (η_{EtOH}). Dividing specific viscosity (η_{sp}), expressed as η_{rel}–1, by the concentration of silica (C), the reduced viscosity (η_{sp}/C) can be calculated. Plotting η_{sp} / C vs. C allows insight into the dependence of formation of polymeric silica clusters on silica concentration.

2.2. Sols for the spinning process

According to the spinnability test and the rheological measurements, the sols were considered to be spinnable when the criteria were fulfilled and suitable process conditions were then developed for the spinning process. For practical reasons and in order to save time, the preparation of the spinning solution differs from the

preparation described above. Evaporation of ethanol was used to reduce the overall process time after which all the fibre sols were still spinnable. The initial sol preparation is similar, ethanol was mixed with TEOS and nitric acid with water. The acid/water solution was added to the TEOS/ethanol solution under vigorous stirring and then the solution was poured into an evaporating dish. The lid of the dish is a special cooler which condenses the evaporating ethanol and leads it off to a volumetric flask. The evaporating dish was placed into a water bath (40°C) and the solution was kept there (20–22 h) until a certain amount of the sol had evaporated. Table 2 shows theoretical silica concentrations assuming the net reaction and that the evaporating fraction consists mostly of ethanol as a result of the relatively low temperature and low water content ($r = 1$) that is mostly consumed in hydrolysis. The recipe for FIB1 was additionally prepared at 75°C to test the spinnability. The sols were cooled to either 20 or 0°C (depending on the sample). When the spinning solution reached a certain level of viscosity, spinning was started. A rotational viscometer with a disc shaped spindle (Brookfield LVDV II+) was used to define the point where the spinning could be started. Because of practical problems due to the substantial batch size of the spinning sols, the obtained viscosity values were not absolute, but comparable to each other. The initial viscosity was the same for all sample sols when the spinning process was started. However, each sol recipe was used to spin fibres in two stages (A and B). The starting viscosity was 1.5–2 times higher in the second stage. Air bubbles were removed from the spinning solution under partial vacuum. If this is not done the sol–gel filaments will break due to a discontinuous flow of the spinning solution.

Dry spinning was used to prepare the sol–gel fibres. The spinning solution was kept in a container whose temperature was adjustable. Nitrogen gas was led into the closed container to push the spinning solution to a gear pump. Nitrogen is a good choice for this purpose because the spinning solution is isolated from contact with humid air. The gear pump (Zenith 958736) with a capacity of 0.6 ml/revolution metered the spinning solution to the spinning head. The spinneret is made of a gold/platinum alloy. The diameter of the holes was 0.065 mm and the l/d ratio was 1. The number of the holes was 6. The distance between the spinneret and the wind-up roll was adjusted to meet the demands of each fibre.

Table 2
Silica content of the spinning solution

Sample name	$m(SiO_2)/[m(SiO_2)+m(EtOH)]$(wt%)
FIB1_A	45.4
FIB1_B	45.4
FIB2_A	42.7
FIB2_B	42.7
FIB3	41.7

2.3. Characterisation of fibres

The infrared absorption spectra were recorded between 400 and 4000 cm^{-1} using Bruker IFS 66 FTIR spectrometry. The measurements were carried out with the diffuse reflectance infrared fourier transformation (DRIFT) system. Potassium bromide was used as a background material. The resolution of the FTIR equipment was 4 cm^{-1}.

A thermogravimetric analysis (TGA) was performed on the green state fibres to measure weight changes with a Netzsch TG-209 equipment (NETZSCH GmbH, Selb, Bavaria, Germany) with nitrogen as the protective gas and air as the purge gas. The sample holder was a ceramic alumina crucible and the background measurement was done with an empty crucible before the measurements. The mass loss during the heat-treatment of the fibres was measured with a temperature program including several steps, both isothermal and dynamic: isothermal for 15 min at 21°C, dynamic 21–150°C with 2°C/min, isothermal for 60 min at 150°C, dynamic 150–700°C with 5°C/min and isothermal at 700°C for 30 min.

The biodegradation of the samples was studied in vitro using a so called simulated body fluid (SBF).[34] The simulated body fluid was prepared by dissolving reagent chemicals of NaCl (Riedel-de Haën, 31434), $NaHCO_3$ (MERCK, 1.06329.0500), KCl (MERCK, 1.04936.0500), $K_2HPO_4{\cdot}3H_2O$ (MERCK, 1.05099.0250), $MgCl_2{\cdot}6H_2O$ (MERCK, 1.05833.0250), $CaCl_2{\cdot}2H_2O$ (MERCK, 1.023 82 0500) and Na_2SO_4 (MERCK, 1.06649.0500) into deionised water. The fluid was buffered at physiological pH 7.40 at 37°C with tris(hydroxymethyl)-aminomethane (SIGMA®.TRIZMA® BASE, 1503) and hydrochloric acid (MERCK, 100 317). The exact formulation of SBF is given in Table 3.

Three pieces of each specimen were used to investigate the reactions of the sol–gel derived silica fibres in SBF. Each sample (10 mg) was immersed in 50 ml of SBF contained in a polyethylene bottle covered with a tight lid. Three samples of SBF enclosed in bottles without a specimen were used as controls to examine the solution stability. The samples were immersed in the SBF fluid for 2 weeks, the bottles being placed in a shaking water bath (SBD 50 (shake 2: 36 mm (length of stroke), speed = 160 strokes per minute) having a constant temperature at 37°C.

Sample solutions were monitored for silicon and calcium concentrations as a function of immersion time. Calcium concentrations were determined with an atomic absorption spectrophotometer (AAS, Perkin-Elmer 460). Silicon concentrations were analysed by a molybdenum blue-method[35] based on reduction with

Table 3
Reagents for preparing the SBF[34] and ion concentrations of SBF and human blood plasma

Order	Reagent	Amount/1dm3 (H_2O)	Ion	Concentration (mM)	
				Simulated fluid	Human plasma
1	$(CH_2OH)_3CNH_2$	6.055 g	Na^+	142.0	142.0
2	NaCl	7.995 g	K^+	5.0	5.0
3	$NaHCO_3$	0.353 g	Mg^{2+}	1.5	1.5
4	KCl	0.224 g	Ca^{2+}	2.5	2.5
5	$K_2HPO_4{\cdot}3H_2O$	0.228 g	Cl^-	147.8	103.0
6	$MgCl_2{\cdot}6H_2O$	0.305 g	HCO_3^-	4.2	27.0
7	$CaCl_2{\cdot}2H_2O$	0.368 g	HPO_4^{2-}	1.0	1.0
8	Na_2SO_4	0.071 g	SO_4^{2-}	0.5	0.5
9	2 mol/dm^3 HCl	20 ml	pH at 37°C	7.4	7.4

1-amino-2-naphtol-4-sulfonic acid using a UV–vis spectrophotometer (Hitachi Model 100-60). All samples were tested three times each in order to avoid inaccuracy problems and possible degradation differences depending on the distribution in the cross-sectional diameter of the fibres (30–80 μm, medium value 50 μm).

A scanning-transmission electron microscopy (JEOL, JEM 1200 EX) was used to study the bulk structure of the green state fibres. The fibres were embedded in an epoxy resin (EPON 812). Propylene oxide was used as a solvent and epoxy embedding media DMP-30 and DDSA or MNA as an accelerator and hardeners (FLUKA), respectively. The hardened samples were cut with an ultramicrotome to a thickness of 60–70 nm and the cross sections of the fibres were analysed.

3. Results

3.1. Spinnability of sols

The first goal in the characterisation was to determine the spinnability of the prepared sols in general. The approximate reaction times to reach spinnability in a closed vessel at 40°C for the three prepared fibre sols are shown in Table 4, as well as the approximate spinnability times at room temperature (~25°C). As seen, there are quite big differences between the reaction times although the compositions vary only a little as shown earlier in Table 1. In FIB1 and FIB2, the water-to-TEOS ratio is the same, only the concentration of the catalyst (HNO_3) is higher in FIB2. Both systems seem to work quite well and the spinnability times are long enough to design a practically successful spinning process. The addition of NH_3 in FIB3 had an expected influence. The reaction was clearly faster. Consistent results for the spinnability times were thus obtained. The overall reaction kinetics also controls the spinnability times. They are longer when the reactions are slower.

Table 4
Spinnability times for the sols prepared at 40°C

Sample name	Reaction time until spinnable (h)	Spinnable at RT (h)
FIB1 (A and B)	400–450	>8
FIB2 (A and B)	210–215	5–7
FIB3	68–69	3–4

The summary of the rheological measurements is shown in Fig. 1. The reduced viscosity is low for every sol and it increases only gradually with the reaction time. Additionally, the reduced viscosity becomes clearly dependent on the silica concentration only at t/t_{gel} ~0.95. None of the fibre sols were spinnable before the relative gel time t/t_{gel} ~0.95 was achieved. This behaviour of the sols indicates a typical process for linear silica cluster formation, where the condensation kinetics is relatively slow, the degree of branching of the silica clusters is low and the viscosity gradually increases without gel formation.

All sample sols were also spinnable after the EtOH evaporation in the dry spinning. The filament qualities are described in Table 5. The fibres spun in the early stage of the spinnability and FIB3 were processed at 0°C to reach a suitable viscosity level. Recipe for FIB1 was additionally prepared at 75°C and the spinnability was found to be good. The fibre diameters were between 30 and 70 μm the average being about 50 μm for every sample.

3.2. Fibre structure

In order to find out something about the bulk structure of the fibres, a thermogravimetric analysis (TGA) was performed for the fibres aged in a desiccator at room temperature for 3 months. The analysis was done up to 700°C because higher temperatures are practically useless concerning biodegradable applications of silica fibres. The results including the corresponding differential curves are shown in Fig. 2. The physical appearance of the fibres and the quality of the fibre filament in the spinning process, shown in Table 5, seem to correlate with the TGA measurements. In general, one can

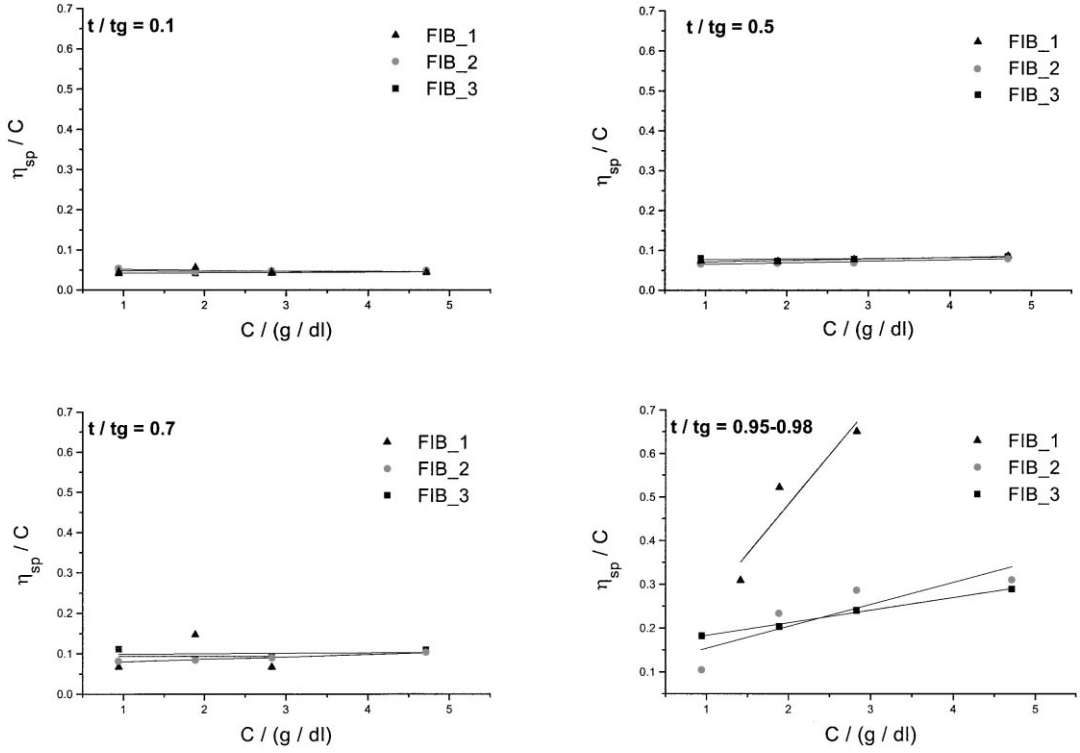

Fig. 1. The reduced viscosity as a function of silica concentration at different relative gel times for the sols prepared at 40°C.

Table 5
Filament quality in spinning and physical appearance after heat treatment

Sample name	Filament quality	Physical appearance
FIB1_A	Poor	Black
FIB2_A	Poor	Black
FIB1_B	Good	White
FIB2_B	Good	White
FIB3	Intermediate	Brown

say that the mass losses are quite considerable (15–25%), which stresses that a careful control of the heat treatment is required in order to avoid cracking problems. The mass loss of the fibres spun in the early stage of spinnability is not so great as that of those spun in the later stage of spinnability. The greatest difference starts to happen at about 300°C, where the organic matter usually starts to evaporate. Because the recipe is exactly the same for FIB1_A and FIB1_B, as well as for FIB2_A and FIB2_B, respectively, it is likely that some organic matter is captured in the fibre structure in the fibres spun in the early stage. Also the shift observed in the differential curves of the fibres spun in the later stage of spinnability (FIB1_B, FIB2_B and FIB3) indicates some differences in the evaporation of the organic matter and in the fibre structure. The physical appearance of the fibres contributes suggestions. The black colour of the fibres spun in the early stage of spinnability indicate that they contain carbon residuals. FIB3, where

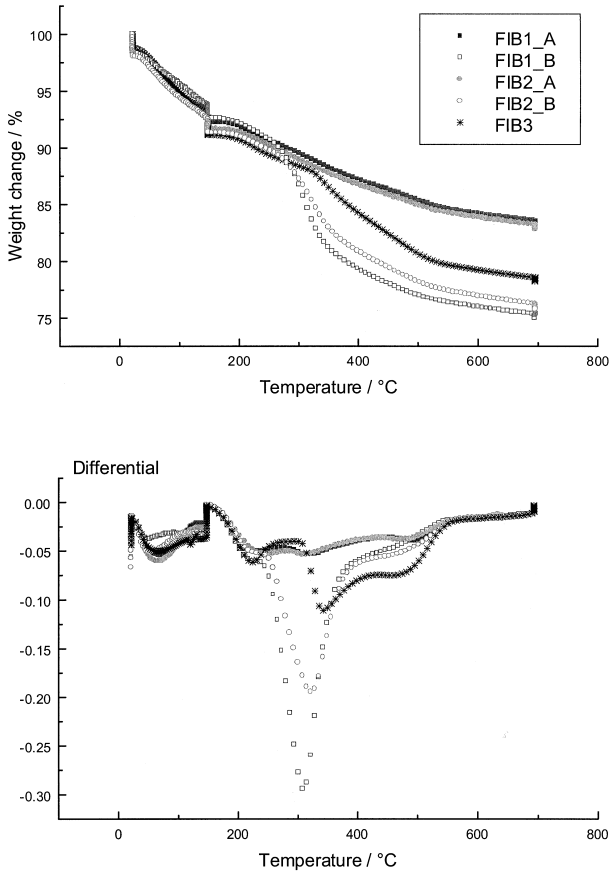

Fig. 2. Thermogravimetric spectra including the corresponding differential curves for the green state fibre samples aged for 3 months.

both HNO_3 and NH_3 were used as catalysts, has intermediate properties, both in the TG analysis and in physical appearance. The mass loss is greater than in FIB1_A and FIB2_A, but smaller than in FIB1_B and FIB2_B. Also the colour of the fibre is something between white and black, i.e. brown. Also the filament quality in the spinning process has analogous properties. The best continuous fibres are achieved with FIB1_B and FIB2_B. One has some difficulties with FIB3, FIB1_A and FIB2_A (processed at 0°C to achieve high enough viscosity in spinning). The filament easily breaks and continuous fibre processing is more difficult.

The FT–IR measurements made for the fibres heat-treated in the thermogravimetric analysis are shown in Fig. 3. They give further contribution for the suggestions made above. The measurements give information of the typical OH groups on the silica surface, but also two unusual peaks are detected in the fibres spun in the early stage of spinnability (FIB1_A and FIB2_A). These interesting peaks at 2330 and 3050 cm^{-1} are clearly seen only for FIB1_A and FIB2_A, but they cannot be directly related to any component present in the system. The only possibility is, that the fibres contain carbon residuals which may form double bonds with hydrogen (3050 cm^{-1}) and oxygen (2330 cm^{-1}) observed at these points. The broad peak at 3400 and 3770 cm^{-1} includes peaks related to isolated single SiOH groups, isolated geminal groups, H-bonded hydroxyls and physically adsorbed water which additionally has a peak at approximately 1630 cm^{-1} (broad). Additionally, the shift in the peaks indicated by the cross-reference line drawn in the graph suggest that some organic residuals also are detected here. The shift is analogous with the extra peaks observed for FIB1_A and FIB2_A and the slight shift for FIB3 is consistent with the intermediate physical appearance. Peaks related to Si–O–Si vibrations are observed at 1200–1100 (broad) and 800 cm^{-1}. The peaks at 1870 and 2000 cm^{-1} are the Si–O–Si overtone bands of silica. The peak at 1300–1400 cm^{-1} is not typical for silica, but NO_3^- stretching vibration is typically located there. The used catalyst in the sol preparation process was HNO_3, which may have left residuals. The fibre structure is commonly condensed and the temperature increased from 450 to 700°C quite quickly and was kept there only for 30 min. It means that the decomposition of nitrate is not very effective.

Transmission electron microscopy was used to illustrate the pore structure of the fibres. Also another method was tested; N_2-sorption measurement, but it was not very practical, because the heat-treatment at ca. 500°C had to be done (in this case) to get any reasonable results from the sorption measurements. In addition, we know that the biodegradation ceases remarkably already after heat-treatment at 300°C. The transmission electron micrograph of the cross-section of FIB2_B is shown in Fig 4. The image was chosen as an example to show the inner structure of the sol–gel derived silica fibre. The images of all five samples resemble each other. FIB2_B is suggested to be a representative example of the fibres because the filament quality was good and the fibres were easy to prepare.

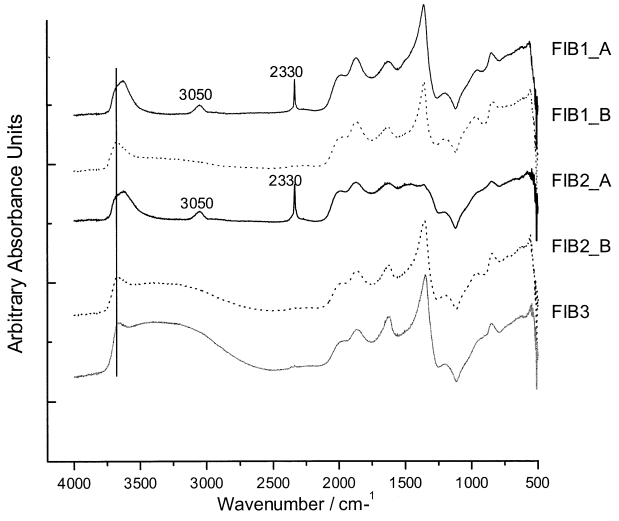

Fig. 3. FT–IR spectra for the fibre samples heat-treated in the thermogravimetric analysis.

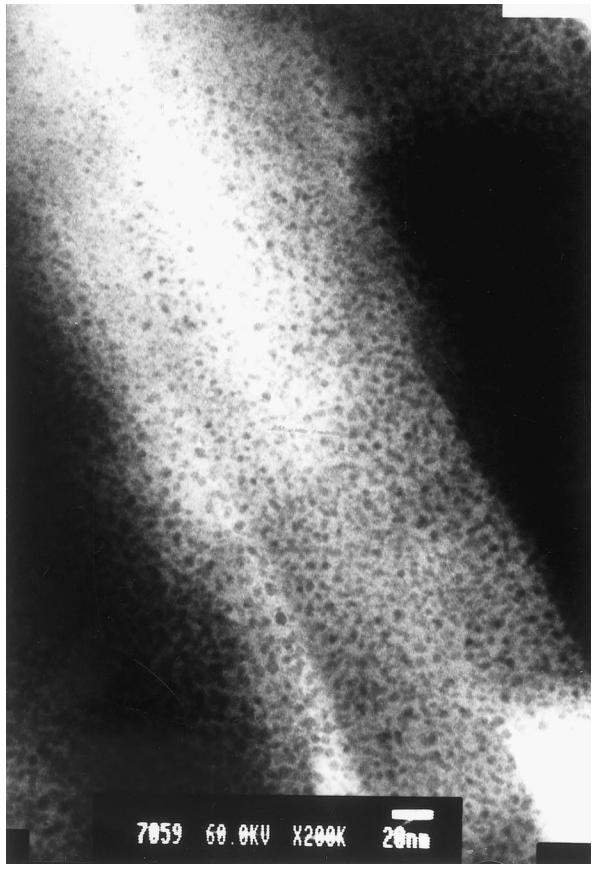

Fig. 4. A transmission electron micrograph for the green body of FIB2_B aged for 3 months.

The white bar at the bottom of the image corresponds 20 nm. The structure is typical for sol–gel derived materials. The structure is not completely condensed, but it contains a lot of small pores of about 2–5 nm in diameter, which indicates that structure is formed from smaller silica units.

3.3. Biodegradation of fibres

The biodegradation data (in vitro in the simulated body fluid) of the green state fibres aged for about one and three months are summarised in Figs. 5 and 6, respectively, and in Table 6. The same kind of analogy

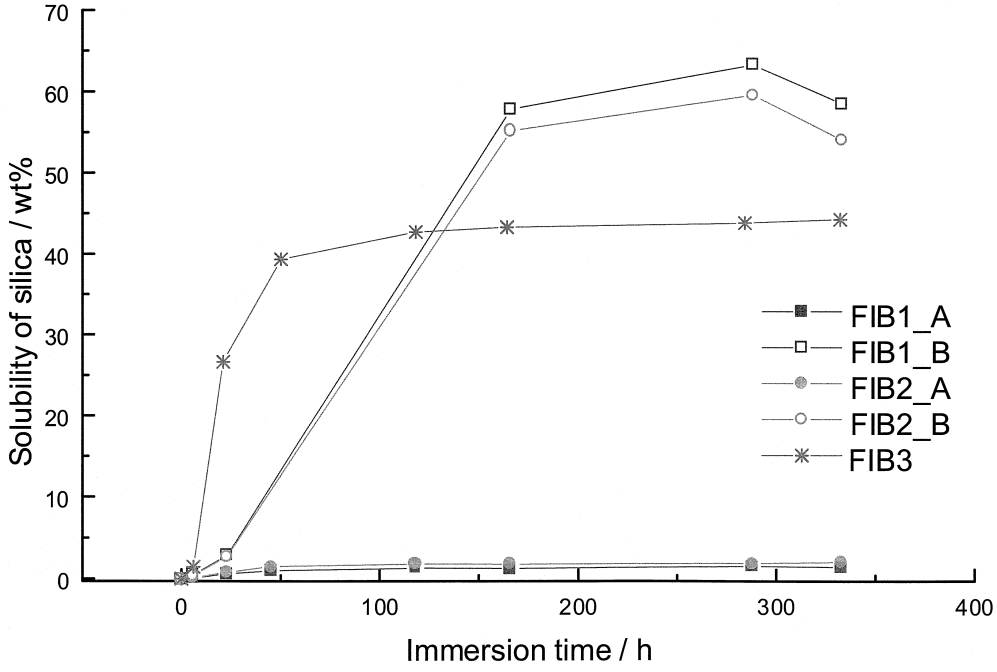

Fig. 5. Biodegradation of the green state fibres aged for 1 month.

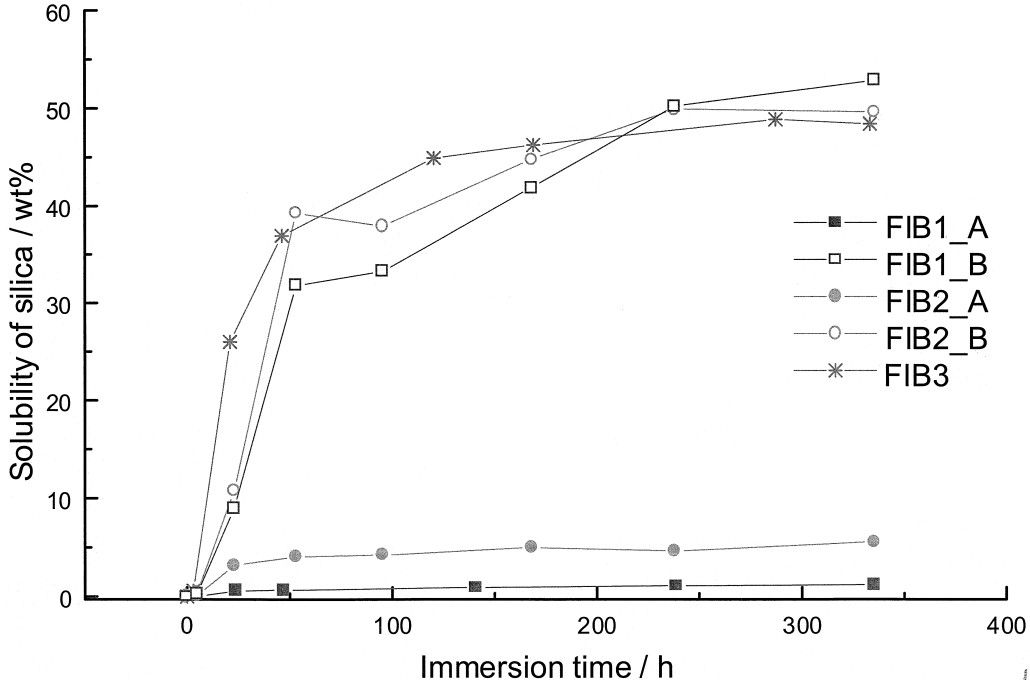

Fig. 6. Biodegradation of the green state fibres aged for 3 months.

Table 6
Silica solubility of the fibres soaked in the SBF

Fiber name	Aging time/months	Silica solubility in SBF/wt%/h[a]
FIB1_A	1	0.02
FIB2_A	1	0.03
FIB1_B	1	(0.8)[b]
FIB2_B	1	(0.9)[b]
FIB3	1	1.7
FIB1_A	3	0.03
FIB2_A	3	0.2
FIB1_B	3	0.7
FIB2_B	3	0.8
FIB3	3	1.4

[a] Calculated from the linear portion of the curves before the saturation level between 5 and 53 h of immersion.
[b] Estimation, the point at ~50 h is missing due to technical problems.

as observed in the TG analysis and in the FT-IR measurements is also observed here. The fibres spun in the early stage of spinnability (FIB1_A and FIB2_A) degrade very slowly as compared to fibres spun in the later stage (FIB1_B, FIB2_B) FIB3 again having some kind of intermediate properties. According to the results obtained, it is typical that some kind of plateau value or a saturation level is achieved after a few days of immersion in the simulated body fluid. The solubility rates (before the plateau level) of FIB1_B, FIB2_B and FIB3 are clearly faster than for FIB1_A and FIB2_A. This indicates that in the structure of the fibres spun in the later stage of spinnability, the area of silica available for the degradation has to be greater. As observed in Table 6, there are some differences in the degradation if the samples aged for 1 or 3 months are compared to each other. For FIB2_A a clear difference is observed. The rate of solubility is greater, as is the silica saturation level (~2 % for the sample aged for 1 month and ~5% for the sample aged for 3 months). For the fibres spun in the later stage (FIB1_B, FIB2_B and FIB3) there are no significant differences after 1 or 3 months of ageing. The values are practically the same indicating that the structures are quite stable. However, they all are clearly more soluble in the SBF than the fibres spun in the early stage of spinnability.

4. Discussion

The tests with the glass rod-method and rheological measurements gave expected spinnability results for the recipes utilised in this study. The test with the glass rod-method is naturally an approximate procedure to determine the spinnability and it does not tell much about the filament quality in the spinning process, but it is considered to be a relatively reliable first check for the rheological characterisation of the sols. The results are in accordance with earlier studies of spinnability[3,4,7,15] indicating the presence of linear polymer structures near the gel point. A low water-to-alkoxide ratio (r) seems to be the only significant factor effectively preventing the functionality and keeping the silica clusters linear. The addition of NH_3 did not destroy the spinnability although it catalyses the condensation reactions and may thus enhance a bit the functionality of the silica precursors. The same conclusion is made about the evaporation of ethanol. Although the circumstances were different in the dry spinning (as compared to rheological measurements for the sols only), the enhanced reaction from the evaporation of ethanol does not seem to have an influence on the spinnability and neither did the enhanced temperature (75°C) for FIB1. Because of this, one is able to design process conditions and times that can easily be adjusted. This could be useful for process design of the sol–gel derived fibres to fit the overall reaction kinetics when other components are used as additives or composite parts. The additives (for example organic medicines) may be sensitive to the process conditions or amount of liquid, which is used as a solvent (for example alcohol or higher temperatures) or they may need time to be dissolved to a desirable form before the next process step can be started.

The TEM image showed that the fibre bulk structure is not completely condensed despite the macroscopic appearance. It has a typical structure of silica sol–gel derived material prepared in an acidic sol containing small pores. However, the method is too insensitive to provide any reliable quantitative explanations for differences in the bulk structure.

The thermogravimetric analysis indicates much evaporation from the bulk during the heat-treatment of the fibres. The temperature program was designed to be quite fast and the temperatures relatively low because the biodegradation of the fibres disappears during long heat-treatments as the structure is sintered. Clear differences are seen, although no thermal equilibria at certain temperatures was implied. Up to 150°C the fibres behave similarly and at 150°C (isothermal for 60 min) no mass loss was detected, which indicates earlier removal of water from the bulk structure. However, if the fibres are heat-treated at temperatures below 300°C, organic matter remains in the structure and the differences between different fibre samples are remarkable. In the case of the fibers spun in the early stage of spinnability, the mass loss of organic matter is clearly lower than that of the fibres spun in the later stage and the colour of the fibres after the heat-treatment contributes the same conclusion about the organic residuals. The reason for this is suggested to be in the fibre bulk structure. If the organic matter has been captured into the silica structure, a more porous silica structure allows the organic components to be removed from the structure easier than from a condensed structure. The FT–IR measurements support the suggestions made for

the TG analysis. There are differences in the bulk structure. Extra peaks are seen for the fibres spun in the early stage of spinnability indicating organic residuals in the otherwise typical silica structure.

Analogous results contributing suggestions about the bulk structure were obtained in the biodegradation experiments. They also indicate differences in the structure. For the fibres spun in the later stage of spinnability, the area of silica available for degradation has to be greater. There are two possible reasons for this. The first one is possible differences in the silica bulk structure. More porous structures of the same material degrade faster than corresponding condensed material. The other one is possible differences in the bulk structure caused by the organic residuals which are less soluble or insoluble in the simulated body fluid and in that way prevent or retard the degradation of silica by plugging the pores. However, as mentioned in the TGA and FT–IR results, the condensed silica structure and the amount of the organic residuals also may have a direct dependence on each other. The condensed silica structure captures the organic residuals and more energy is needed for the evaporation meaning that the condensed silica matrix alone may be responsible for the slower degradation. Additionally, as the simulated body fluid is used, there is always a possibility that the materials are bioactive (a special type of calciumphosphate, bone-like hydroxyapatite is formed on the bioactive surface), meaning that the formed calciumphosphate surface layer works as a preventing layer on top of the silica. However, the concentration of the calcium species was determined and some decrease in calcium concentration was observed in some samples, but not until 7–10 days of immersion in the simulated body fluid. In turn, the saturation level is achieved in few days meaning that the decrease in the calcium (which indicates possible bioactivity in vitro) concentration does not have an influence on the silica solubility.

The differences in the biodegradation of the fibres aged for 1 or 3 months were not remarkable, except in the case of FIB2_A (spun in the early stage of spinnability). The recipe of FIB2 (A and B) contains quite a lot of catalyst (HNO_3). It has to be remembered that the aged fibres are green state fibres and not heat-treated and the used water amount is low (stoichiometrical) so that the reactions are not complete at the gel point. The organic remains in the green state fibres are remains of TEOS and they have a good chance and time (2 months) to continue reactions especially when the catalyst concentration has been quite high. The differences in the biodegradation results depend again either on the amount of the organic remains or on the silica bulk structure which may change as the unreacted components continue to react.

As noted, the reasons for achieving different bulk structures are more or less dependent on each other. As the different recipes are compared to each other, it is obvious that the concentrations of the precursors have an influence on the silica cluster structure and on the green state bulk structure. But because the sols are spinnable and spun at $t/t_g = 0.95$–0.98, it is assumed that the degree of TEOS hydrolysed and condensed cannot directly have a significant influence on differences of the organic remains in the structure of the fibres made with the same recipe and aged similarly. However, it is obvious that the silica bulk structures are different and so is the release of the organic matter during the heat-treatment. As mentioned earlier in the results, the filament quality was more difficult to control for the fibres spun in the early stage of spinnability. Although the viscosity of the sol is high enough to spin fibres in both cases, it is also naturally lower at $t/t_g = 0.95$ than for example at $t/t_g = 0.98$. In the case of FIB3 (spun quite near the gel point), a high enough viscosity was achieved only by adjusting the temperature to 0°C in order to be able to do the dry spinning in practice. The spinning time was very short and very near the gel point at the room temperature. This also indicates that the sol may be ready-made for the spinning with respect to the linear silica cluster structure although the viscosity is not high enough. Besides temperature, the viscosity value depends on the polymer concentration, chain length and form in the sol, which in turn depend on the reaction circumstances indicating that many factors depending on each other have to be taken into account to prepare controlled fibres. However, the absolute viscosity value alone may have a decisive role in the formation of the different bulk structures. It may have an influence on the orientation of the silica polymers during the spinning. A higher viscosity inhibits the orientation leaving the structure more branched. Another possibility is that the silica polymers are somewhat smaller in the earlier stage of spinnability and they are simply packed better than larger polymers in the later stage of spinnability.

A sintering study and careful surface characterisation would be natural choices to continue the research work in order to develop and optimise the functionality of the fibres concerning biodegradation and mechanical properties. The combination of the different green state fibre structures and heat-treatments provides interesting possibilities to prepare an assembly of fibres for different bioceramics applications.

5. Conclusions

The fine adjustments of the recipes had a slight influence on the biodegradation, but the sol–gel process stage had a much stronger influence. During the process stage when the sols are spinnable, different spinning moments for the same sol can be utilised to adjust biodegradation of sol–gel derived silica fibres. The fibres

spun in the early stage of the spinnability degrade more slowly in the simulated body fluid. A silica sol may coincidently be spinnable with respect to the linear silica cluster structure but not with respect to the viscosity. The spinnability is achieved by controlling the viscosity level by enhancing or lowering the temperature of the sol. Addition of NH_3 into the sol pre-catalysed by an acid did not destroy the spinnability, but the reaction time is reduced remarkably. Evaporation of ethanol or enhanced reaction temperature did not have an influence on the spinnability as compared to the corresponding samples kept in closed vessels, only reaction times were reduced. This provides a good way to control the total time of the preparation process. If the fibres are heat-treated at temperatures below 300°C, the differences in the fibre bulk structures are remarkable. Ageing of the fibres did not have a remarkable influence on the biodegradation, except in the case of greater amount of catalysts used in the preparation of the sol. By combining the concentrations of substances, process stage, reaction circumstances and the viscosity of the sol properly, different green state fibre structures with adjustable biodegradation can be prepared.

Acknowledgements

Technology Development Centre of Finland (TEKES) is acknowledged for financial support. The authors also wish to thank Dr. Jouko Mäki for his assistance in TEM measurements.

References

1. Hench, L. L., Bioceramics: from concept to clinic. *J. Am. Ceram. Soc.*, 1991, **74**, 1487–1510.
2. Hench, L. L. and Wilson, J., *Introduction to Bioceramics*. World Scientific Publishing Co. Pte. Ltd, USA, 1993.
3. Sakka, S. and Kamiya, K., The sol–gel transition in the hydrolysis of metal alkoxides in relation to the formation of glass fibers and films. *J. Non.-Cryst. Sol.*, 1982, **48**, 31–46.
4. Sakka, S. and Kozuka, H., Rheology of sols and fiber drawing. *J. Non.-Cryst. Sol.*, 1988, **100**, 142–153.
5. Kozuka, H., Kuroki, H. and Sakka, S., The change of flow characteristics of $Si(OC_2H_5)_4$ solutions in the course of sol–gel conversion. *J. Non.-Cryst. Sol.*, 1988, **101**, 120–122.
6. Sowman, H. G., A new era in ceramic fibers via sol–gel technology. *Cer. Bull.*, 1988, **67**, 1911–1916.
7. Brinker, C. J. and Assink, R. A., Spinnability of silica sols. *J. Non.-Cryst. Sol.*, 1989, **111**, 48–54.
8. Matsuzaki, K., Arai, D., Taneda, N., Mukaiyama, T. and Ikemura, M., Continuous silica glass fiber produced by sol–gel process. *J. Non.-Cryst. Sol.*, 1989, **112**, 437–441.
9. Ro, J. C. and Chung, I. J., The rheology of silica sols during the gelation process. *J. Non.-Cryst. Sol.*, 1990, **126**, 259–266.
10. Brinker, C. J. and Scherer, G. W., *Sol–Gel Science: The Physics and Chemistry of sol–gel Processing*. Academic Press, San Diego, CA, USA, 1990 pp. 204–209.
11. Kamiya, K. and Hashimoto, T., The sol–gel process for making SiO_2 glass fibres from $Si(OC_4H_9)_4$–H_2O–C_2H_5OH–HCl solutions — comparison with $Si(OC_2H_5)_4$ solutions. *J. Mat. Sci. Lett.*, 1990, **9**, 1341–1344.
12. Brenna, U., Carturan, G. and Sorarù, G. D., Rheological behaviour of solutions affording SiO_2 and SiO_2/ZrO_2 fibers. *J. Non-Cryst. Sol.*, 1991, **134**, 191–198.
13. Zhou, W., Xu, Y., Zhang, L. and Sun, X., Crystallization of silica fibers made from metal alkoxide. *Mat. Lett.*, 1991, **11**, 352–354.
14. Hashimoto, T., Kamiya, K. and Nasu, H., Strenthening of sol–gel-derived SiO_2 glass fibers by incorporating colloidal silica particles. *J. Non-Cryst. Sol.*, 1992, **143**, 31–39.
15. Sakka, S. and Yoko, T., Fibers from gels. *J. Non.-Cryst. Sol.*, 1992, **147 and 148**, 394–403.
16. Pozo de Fernandez, M. E., Kang, C. and Mangonon, P. L., Process ceramic fibers by sol–gel. *Chem. Eng. Prog.*, 1993, **9**, 49–53.
17. Shin, D. and Han, S., Spinnability and rheological properties of sols derived from $Si(OC_2H_5)_4$ and $Zr(O–nC_3H_7)_4$. *J. sol–gel Sci. Tech.*, 1994, **1**, 267–273.
18. Sakka, S., Sol–gel processing of insulating, electroconducting and superconducting fibers. *J. Non.-Cryst. Sol.*, 1990, **121**, 417–423.
19. Del Olmo, L. and Caldaza, M. L., $PbTiO_3$ ceramic fibres prepared from a sol–gel process as piezoelectric materials. *J. Non.-Cryst. Sol.*, 1990, **121**, 424–427.
20. Yoko, T., Kamiya, K. and Kanaka, K., Preparation of multiple oxide BaTiO3 fibres by the sol–gel method. *J. Mat. Sci.*, 1990, **25**, 3922–3929.
21. Katayama, S. and Sekine, M., Fabrication of superconducting $YBa_2Cu_3O_{7-x}$ fibers by the sol–gel method using metal alkoxides. *J. Mat. Res.*, 1991, **6**, 1629–1633.
22. Venkatasusubramanian, N., Wade, B., Desai, P. and Abhiraman, A. S., Synthesis and characterization of spinnable sol–gel derived polyborates. *J. Non.-Cryst. Sol*, 1991, **130**, 144–156.
23. Selvaraj, U., Prasadarao, A. V., Komarneni, S., Brooks, K. and Kurtz, S., Sol–gel processing of $PbTiO_3$ and $Pb(Zr_{0.52}Ti_{0.48})O_3$ fibers. *J. Mat. Res.*, 1992, **7**, 992–996.
24. Yogo, T. and Iwahara, H., Synthesis of α-alumina fibre from modified aluminium alkoxide precursor. *J. Mat. Sci.*, 1992, **27**, 1499–1504.
25. Seddon, A. B., Applicability of sol–gel processing in production of silica based optical fibres. *Mat. Sci. Tech.*, 1993, **9**, 729–736.
26. Emig, G., Fitzer, E. and Zimmerman-Chopin, R., Sol–gel process for spinning of continuous (Zr, Ce)O_2 fibers. *Mat. Sci. Eng.*, 1994, **A189**, 311–317.
27. Emig, G., Wirth, R. and Zimmermann-Chopin, R., Sol/gel-based precursors for manufacturing refractory oxide fibres. *J. Mat. Sci. Lett.*, 1994, **29**, 4559–4566.
28. Chiou, Y. H., Tsai, M. T. and Shih, H. C., The preparation of alumina fibre by sol–gel processing. *J. Mat. Sci.*, 1994, **29**, 2378–2388.
29. Narang, U., Gvishi, R., Bright, F. V. and Prasad, P. N., Sol–gel-derived micron scale optical fibers for chemical sensing. *J. sol–gel Sci. Tech.*, 1996, **6**, 113–119.
30. Glaubitt, W., Watzka, W., Scholz, H. and Sporn, D., Sol–gel processing of functional and structural ceramic oxide fibers. *J. sol–gel Sci. Tech.*, 1997, **8**, 29–33.
31. Hasegawa, I., Nakamura, T., Kajiwara, M. and Motojima, S., Synthesis of silicon carbide fibers by sol–gel processing. *J. sol–gel Sci. Tech.*, 1997, **8**, 577–579.
32. Toyoda, M., Hamaji, Y. and Tomono, K., Fabrication of $PbTiO_3$ fibers by sol–gel processing. *J. sol–gel Sci. Tech.*, 1997, **9**, 71–84.
33. Muralidhadran, B. G. and Agrawal, D. C., Sol–gel derived TiO_2–SiO_2 fibres. *J. sol–gel Sci. Tech.*, 1997, **9**, 85–93.
34. Ohtsuki, C., Kokubo, T. and Yamamuro, T., Mechanism of apatite formation on $CaO–SiO_2–P_2O_5$ glasses in a simulated body fluid. *J. Non.-Cryst. Sol.*, 1992, **143**, 84–92.
35. Koch, O. G. and Koch-Dedic, G. A., Siliconmolybdänblau-Verfahren. In *Handbuch der Spurenanalyse*. Springer-Verlag, Berlin, 1974, p. 1105.